Int. J. Radiation Oncology Biol. Phys., Vol. 72, No. 5, pp. 1347–1354, 2008

0360-3016/08/$–see front matter

doi:10.1016/j.ijrobp.2008.03.055

CLINICAL INVESTIGATION **Brain**

SPINAL RECURRENCE FROM INTRACRANIAL GERMINOMA: RISK FACTORS AND TREATMENT OUTCOME FOR SPINAL RECURRENCE

KAZUHIKO OGAWA, M.D.,* YOSHIHIKO YOSHII, M.D.,† NAOTO SHIKAMA, M.D.,‡ KATSUMASA NAKAMURA, M.D.,§ TAKASHI UNO, M.D.,‖ HIROSHI ONISHI, M.D.,¶ JUN ITAMI, M.D.,** YOSHIYUKI SHIOYAMA, M.D.,‡ SHIRO IRAHA, M.D.,* AKIO HYODO, M.D.,† TAKAFUMI TOITA, M.D.,* YASUMASA KAKINOHANA, PH.D.,* WAKANA TAMAKI, M.D.,* HISAO ITO, M.D.,‖ AND SADAYUKI MURAYAMA, M.D.*

* Department of Radiology, University of the Ryukyus, Okinawa, Japan; † Department of Neurosurgery, University of the Ryukyus, Okinawa, Japan; ‡ Department of Radiology, Shinshu University, Fukuoka, Japan; § Department of Radiology, Kyushu University, Nagano, Japan; ‖ Department of Radiology, Chiba University, Chiba, Japan; ¶ Department of Radiology, Yamanashi University, Yamanashi, Japan; and ** Department of Radiology, International Medical Center of Japan, Tokyo, Japan

Purpose: To analyze retrospectively the risk factors of spinal recurrence in patients with intracranial germinoma and clinical outcomes of patients who developed spinal recurrence.

Methods and Materials: Between 1980 and 2007, 165 patients with no evidence of spinal metastases at diagnosis were treated with cranial radiotherapy without spinal irradiation. The median follow-up in all 165 patients was 61.2 months (range, 1.2–260.1 months).

Results: After the initial treatment, 15 patients (9.1%) developed spinal recurrences. Multivariate analysis revealed that large intracranial disease (≥4 cm) and multifocal intracranial disease were independent risk factors for spinal recurrence. Radiation field, total radiation dose, and the use of chemotherapy did not affect the occurrence of spinal recurrences. Of the 15 patients who experienced spinal recurrence, the 3-year actuarial overall survival and disease-free survival (DFS) rates from the beginning of salvage treatments were 65% and 57%, respectively. In the analysis, presence of intracranial recurrence and salvage treatment modality (radiotherapy with chemotherapy vs. radiotherapy alone) had a statistically significant impact on DFS. The 3-year DFS rate in patients with no intracranial recurrence and treated with both spinal radiotherapy and chemotherapy was 100%, whereas only 17% in patients with intracranial recurrence or treated with radiotherapy alone ($p = 0.001$).

Conclusion: Large intracranial disease and multifocal intracranial disease were risk factors for spinal recurrence in patients with intracranial germinoma with no evidence of spinal metastases at diagnosis. For patients who developed spinal recurrence alone, salvage treatment combined with spinal radiotherapy and chemotherapy was effective in controlling the recurrent disease. © **2008 Elsevier Inc.**

Germinomas, Spinal recurrence, Radiation, Chemotherapy.

INTRODUCTION

Intracranial germinomas represent 0.5–2.5% of all intracranial tumors and are more common in Japan than in Western countries (1–5). These tumors occur primarily in the pineal or neurohypophyseal regions and most often affect teenagers and young adults. In contrast to intracranial nongerminomatous germ cell tumors, germinomas are one of the most radiosensitive tumors known and are curable by radiotherapy alone (1, 5–13). Although radiotherapy has been the standard treatment for intracranial germinoma for many years, agreement on the optimal management of these tumors has not been reached. One of the major controversies in the management of intracranial germinoma is the use of craniospinal irradiation in patients with no evidence of spinal metastases at diagnosis (14–18).

Recently, several reports have indicated that the incidence of spinal recurrence was found to be too low to warrant routine spinal irradiation. With modern imaging procedures, the proportion of patients presenting with spinal disease at the time of diagnosis is low, and the risk of secondary spinal seeding in germinoma did not exceed 15% in a large series (8, 19, 20). However, the risk factors for spinal recurrence in patients with no evidence of spinal metastases at diagnosis have not been well documented. Moreover, there is minimal information

Reprint requests to: Dr. Kazuhiko Ogawa, Department of Radiology, Graduate School of Medical Science, University of the Ryukyus, 207 Uehara, Nishihara-cho, Okinawa, 903–0215, Japan. Tel: (+81) 98-895-3331 (ext. 2401); Fax: (+81) 98-895-1420; E-mail: kogawa@med.u-ryukyu.ac.jp

Conflict of interest: none.

Received Jan 17, 2008, and in revised form March 11, 2008. Accepted for publication March 12, 2008.

regarding the outcomes of salvage treatment for patients who developed spinal recurrence. In the current study, we reviewed a retrospective and multi-institutional series of 165 patients with intracranial germinoma who had no evidence of spinal metastases at diagnosis and evaluated the risk factors for spinal recurrence and treatment outcomes for patients who developed spinal recurrences after the initial treatment.

METHODS AND MATERIALS

Patient characteristics

A retrospective review of medical records between 1980 and 2007 identified 240 patients with documented intracranial germinoma treated by radiotherapy at the Department of Radiology, University of the Ryukyus Hospital, Kyushu University Hospital, Shinshu University Hospital, Chiba University Hospital, Yamanashi University Hospital, or the International Medical Center of Japan. Of these, 75 patients having spinal metastases at diagnosis or treated with spinal irradiation were excluded, and a total of 165 patients with no evidence of spinal metastases at diagnosis and treated with cranial radiotherapy without spinal irradiation were subjected to this analysis. With regard to the 75 patients treated with spinal irradiation, 68 patients had no evidence of spinal metastases at diagnosis. The majority of these 68 patients were treated with routine craniospinal irradiation regardless of their disease status between 1980 and 1995, and the disease characteristics of these 68 patients, such as the tumor size and the number of tumor, were not significantly different compared with those of 165 patients treated without spinal irradiation.

Table 1 indicates the patient and treatment characteristics of all 165 patients. All patients were evaluated by computed tomography or magnetic resonance imaging (MRI) scans before initial treatment. One hundred and two patients (62%) were diagnosed pathologically; the remaining 63 patients (38%) were diagnosed clinically as having germinoma by clinical and neuroradiologic signs, as described previously (6, 9, 26). For the assessment of spinal metastases at diagnosis, 81 patients (49%) were evaluated by spinal MRI and the remaining 84 patients were evaluated by cerebrospinal fluid cytology or cerebrospinal fluid tumor markers. Forty patients (24%) had multifocal tumors involving more than one intracranial site, and serum human gonadotropin levels were elevated in 34 (21%) patients, who as a group had a median human gonadotropin value of 44 mIU/mL (range, 15–251 mIU/mL). Patients with human gonadotropin levels greater than 100 mIU/mL had pathologically verified germinomas. No patients had elevated alpha-fetoprotein or carcinoembryonic antigen titer.

Table 1. Patient and treatment characteristics (n = 165)

Characteristic	No. of patients
Age (median, 17 y)	
<20 y	109 (66)
≥20 y	56 (34)
Gender	
Female	38 (23)
Male	127 (77)
KPS	
≥70	128 (78)
<70	27 (16)
Unknown	10 (6)
Tumor location	
Pineal	65 (39)
Neurohypophyseal	46 (28)
Thalamus or basal ganglia	14 (9)
Multifocal	40 (24)
No. of tumor	
Single	125 (76)
Multifocal	40 (24)
Maximal tumor size (cm)	
<4	131 (79)
≥4	34 (21)
Serum hCG level	
Normal	131 (79)
High	34 (21)
Pathology	
Verified	102 (62)
Unverified	63 (38)
Spinal MRI evaluation at diagnosis	
Yes	81 (49)
No	84 (51)
Total radiation dose (Gy)	
≤50	131 (79)
>50	34 (21)
Treatment field	
WB/WV ± B	145 (88)
Local	20 (12)
Chemotherapy	
Yes	75 (45)
No	90 (55)

Abbreviations: KPS = Karnofsky performance status; hCG = human chorionic gonadotropin; MRI = magnetic resonance imaging; WB/WV = whole brain/whole ventricle; B = boost.

Data in parentheses are percentages.

Radiotherapy

Details of radiotherapy method were described as previously (21). In brief, radiotherapy was administered using a ^{60}Co teletherapy unit (4 patients), or a 4-, 6-, or 10-MV linear accelerator, and daily fraction sizes of 1.8–2.0 Gy for the primary tumor 5 days per week were mostly used. In most cases, treatment fields were determined using conventional X-ray simulators. For some cases, in an effort to spare normal brain from the high-dose volume of irradiation, computed tomography simulators were also used to boost the primary disease site. Localized-field irradiation was defined as a partial brain field covering the primary tumor with a generous margin, but not including the third ventricle and lateral ventricles.

One hundred three patients (62%) were treated using a radiation field encompassing the whole brain with or without a boost, 42 patients with the whole ventricle with or without a boost, and 20 patients with a localized-field smaller than the whole ventricle (Table 2). The total dose to the primary site ranged from 24 to 59.5 Gy (median, 48.5 Gy), with 7 patients (4%) receiving total doses of >55 Gy because we previously lacked a consensus regarding optimal doses for these tumors, especially for large tumors. Whole-brain doses ranged from 19.5 to 44 Gy (median, 30 Gy), whole-ventricle doses ranged from 24 to 40 Gy (median, 25.2 Gy), and localized-field doses ranged from 24 to 55.8 Gy (median, 40 Gy).

For patients with spinal recurrences, spinal radiotherapy with or without cranial radiotherapy was administered. The method of spinal radiotherapy was described as previously (22). In brief, spinal irradiation was supplemented using a posteroanterior field with single doses of 1.6–2.0 Gy per fraction and five fractions per week.

Chemotherapy

Seventy-five patients (45%) received systemic chemotherapy with a total of one to six courses (median, three courses) during the initial treatment to reduce the total number of radiation doses

Table 2. Radiation field, total radiation dose, and incidences of intracranial and spinal recurrences according to the treatment modality

Treatment modality	Radiation field	Total radiation dose (range) (Gy)	No. of pts.	No. of low-risk group for SR*	No. of intracranial recurrence	No. of spinal recurrence
RT alone						
	WB ± B	50 (38–59.5)	77	18	1	5
	WV ± B	45 (40–52)	4	0	2	1
	Local	48 (24–55.8)	9	0	3	2
	Total	50 (24–59.5)	90	18 (20%)	6 (7%)	8 (9%)
RT + CT						
	WB ± B	49 (30–55)	26	10	2	4
	WV ± B	30 (24–50)	38	15	1	3
	Local	30 (24–40)	11	0	1	0
	Total	40 (24–50)	75	25 (33%)	4 (5%)	7 (9%)
Total		48.5 (24–59.5)	165	43 (26%)	10 (6%)**	15 (9%)**

Abbreviations: RT = radiotherapy; CT = chemotherapy; WB = whole brain; WV = whole ventricle; B = boost; SR = spinal recurrence; MRI = magnetic resonance imaging.

* Defined as patients with spinal MRI stage negative, small tumor (<4 cm), unifocal tumor, and treatment with WB or WV.

** Four patients developed both intracranial and spinal recurrences.

or radiation fields (Table 2). In patients with radiotherapy alone (median total dose, 50 Gy), 77 of 90 patients (86%) were treated with whole-brain irradiation with or without boost, whereas in patients with radiotherapy and chemotherapy (median total dose, 40 Gy), only 35% of the patients (26 of 75 patients) were treated with whole brain irradiation with or without boost. In the current study, we did not intend to use chemotherapies to reduce the risk of spinal recurrences for these patients. Of 75 patients, 71 patients (95%) received chemotherapy before radiotherapy; 2 patients during radiotherapy and the remaining 2 patients after radiotherapy. All patients received cisplatin or carboplatin in combination with other agents. The most commonly used regimen was a combination of cisplatin and etoposide (35 patients), and the next most common was a combination of carboplatin and etoposide (28 patients). Nine patients received a combination of ifosfamide, cisplatin, and etoposide and 3 patients received a combination of cisplatin and methotrexate. The remaining 1 patient received cisplatin-vinblastine-bleomycin combination therapy. Cycles were usually repeated every 3–4 weeks. Cisplatin and etoposide therapy consisted of cisplatin (20 mg/m^2) and etoposide (60 mg/m^2) for 5 consecutive days (Days 1–5) (23). In the carboplatin and etoposide therapy group, carboplatin (450 mg/m^2) was given on Day 1 and etoposide (150 mg/m^2) was given for 3 consecutive days (Days 1–3) (24). The ifosfamide, cisplatin, and etoposide regimen consisted of iphosphamide (900 mg/m^2), cisplatin (20 mg/m^2), and etoposide (60 mg/m^2) for 5 consecutive days (25); the combination of cisplatin and methotrexate regimen consisted of 50 mg/m^2 of cisplatin on Day 1 with 3 mg of intrathecal methotrexate twice during initial treatment. The cisplatin-vinblastine-bleomycin regimen consisted of cisplatin (20 mg/m^2) for 5 consecutive days (Days 1–5), vinblastine (4–6 mg/m^2) on Days 1 and 8, and bleomycin (10–15 mg/m^2) on Days 1, 8, and 15 (26).

For patients with spinal recurrences, the chemotherapy regimens described here were administered to patients who received both radiotherapy and chemotherapy as a salvage treatment.

Statistical analysis

The median follow-up time of all 165 patients was 61.2 months (range, 1.2–260.1 months), and no patients were lost to follow-up.

Table 3. Clinical data on 15 patients with spinal recurrence (at initial treatment)

Pts. no.	Age	Gender	Pathologic confirmation	Serum hCG	KPS (%)	Primary tumor site	Maximal tumor size (cm)	Total radiation dose	Radiation field	Use of CT	CT regimen (initial Tx)
1	20	Male	Yes	Normal	100	P+N	2	30	WV	Yes	EP
2	15	Male	Yes	Normal	60	P	5	50	WB+L	No	—
3	27	Male	Yes	Elevated	100	P	3	50	WV+L	Yes	CBDCA+VP16
4	27	Male	No	Normal	100	P	2	46	WB+L	No	—
5	12	Female	Yes	Elevated	90	N	4.5	40	WB+L	Yes	EP
6	10	Female	No	Elevated	100	P+N	4	40	L	No	—
7	2	Female	Yes	Normal	40	P	2.5	20	L	No	—
8	17	Female	Yes	Normal	100	N+D	3	40	WB+L	No	—
9	20	Male	Yes	Normal	90	P+N+D	3	50	WB+L	Yes	CBDCA+VP16
10	16	Male	Yes	Normal	100	P	5	50	WB+L	No	—
11	18	Female	No	Normal	100	P	1.5	50	WB+L	No	—
12	30	Male	Yes	Elevated	100	P+D	4.5	50	WV	Yes	CBDCA+VP16
13	13	Male	No	Normal	100	N+D	4	59.5	WB+L	Yes	CDDP+MTX
14	14	Male	No	Normal	90	N+Pons	4.5	48.5	WB+L	Yes	CDDP+MTX
15	14	Male	Yes	Normal	90	P+N	4	50	WV	No	—

Abbreviations: hCG = human chorionic gonadotropin; KPS = Karnofsky performance status; CT = chemotherapy; Tx = therapy; P = pineal; N = neurohypophyseal; D = dissemination; WB = whole brain; WV = whole ventricle; L = local; EP = cisplatin and etoposide; EP = cisplatin and etoposide; CBDCA = carboplatin; VA-16 = etoposide; MTX = methotrexate.

Table 4. Clinical data on 15 patients with spinal recurrence (at spinal recurrence)

Pts. no.	Age at spinal recurrence	Spinal recurrence site	Intracranial recurrence	Spinal radiation field	Spinal radiation dose (Gy)	Intracranial RT	CT after spinal recurrence	CT regimens after spinal recurrence	No. of cycles of CT	Site of re-recurrence after salvage Tx	Outcome	Follow up
1	24	C2-3	No	WS	30.6	No	Yes	ICE	3	—	NED	46.0 Mo
2	18	Th8-9	No	WS+L	45	No	Yes	ICE	4	—	NED	27.7 Mo
3	28	Th4	Yes	WS+L	30.6	Yes (24 Gy)	Yes	ICE	3	Intracranial	Dead	9.8 Mo
4	43	L1-3	No	WS+L	46	No	Yes	ICE	5	—	NED	193.9 Mo
5	18	Multiple	Yes	WS+L	46	Yes (20 Gy)	Yes	EP	3	Intracranial	AWD	69.6 Mo
6	13	Multiple	No	WS	36.3	No	Yes	CBDCA+VP16	3	—	NED	6.3 Mo
7	2	Multiple	Yes	WS	30.6	No	No	-	-	Intracranial, Spinal	Dead	2.1 Mo
8	24	L2	Yes	WS+L	44	Yes (18 Gy)	Yes	CBDCA+VP16	3	Intracranial	AWD	78.0 Mo
9	25	C5-Th2	No	WS+L	45	No	Yes	ICE	3	—	NED	59.4 Mo
10	17	Multiple	No	WS	24	No	No	-	-	Spinal	Dead	10.3 Mo
11	18	Th6-7, L4	No	WS	30	No	Yes	CBDCA+VP16	3	Intracranial	Dead	87.0 Mo
12	30	Multiple	No	WS	30	No	Yes	CBDCA+VP16	3	—	NED	2.8 Mo
13	14	Multiple	No	WS	33	No	Yes	CBDCA+VP16	3	—	NED	5.6 Mo
14	15	Multiple	No	WS	20	No	No	-	-	Spinal	Dead	17.1 Mo
15	15	Th12-S3	No	WS+L	45	No	Yes	CBDCA+VP16	3	—	NED	8.9 Mo

Abbreviations: RT = radiotherapy; CT = chemotherapy; Tx = therapy; C = cervival spine; Th = thoracic spine; L = lumbar spine; WS = whole spine; L = localized field; ICE = ifosphamide, cisplatin, and etoposide; PE = cisplatin and etoposide; CBDCA = carboplatin; VP-16 = etoposide; NED = no evidence of disease; AWD = alive with disease; Mo = months.

For the assessment of risk factors for spinal recurrence, the chi-square test and logistic regression analysis were used to investigate the relationship between variables and the occurrence of spinal recurrence. For the assessment of treatment outcomes for patients who developed spinal recurrence, overall and disease-free survival (DFS) rates were calculated actuarially according to the Kaplan-Meier method (27) and were measured from the beginning of salvage treatment. Differences between groups were estimated using the log–rank test (28). A probability level of 0.05 was chosen for statistical significance, and statistical analysis was performed using the SPSS software package (version 11.0; SPSS, Inc., Chicago, IL).

RESULTS

After the initial treatment, 10 patients (6%) developed intracranial recurrence and 15 patients (9.1%) developed spinal recurrences (Table 2). The median duration from the date of initial treatment to the date of spinal recurrence was 16.8 months (range, 2.4–199.2 months). Patient and disease characteristics in 15 patients with spinal recurrence were listed in Tables 3 and 4.

As shown in Table 5, the incidence of spinal recurrences was significantly higher in patients with primary large (≥4 cm) tumor at initial diagnosis than those without large tumors. Concerning the maximal tumor size, a cutoff size of 4 cm was used because the incidences of spinal recurrence increased as the tumor size increased, especially to 4 cm or larger (Table 6). Also, the incidence of spinal recurrence was significantly higher in patients with primary multifocal tumor at initial diagnosis compared with those without multifocal tumors. No significant differences were seen with respect to other factors, such as radiation field, total radiation dose, and the use of chemotherapy (Table 5). Of these 40 multifocal primary tumors, 18 tumors were bifocal (pineal and neurohypophyseal), and 3 of 18 patients (17%) with these bifocal germinoma had spinal recurrence after the initial treatment. Multivariate analysis revealed that large intracranial disease and multifocal intracranial disease each were independent risk factors for spinal recurrence (Table 5). We were able to define a low-risk group for spinal recurrence as patients with spinal MRI stage negative, small tumor (<4 cm), unifocal tumor, and treatment with whole-brain or whole-ventricle irradiation (Table 2). None of these 43 patients (0%) in the low-risk group developed spinal recurrence, whereas 15 of 122 patients who did not meet the criteria of the low-risk group (12%) developed spinal recurrence.

Regarding the 15 patients who experienced spinal recurrences, the 3-year actuarial overall survival and DFS rates from the beginning of salvage treatments were 65% and 57%, respectively (Fig. 1). The median total dose to the recurrent spinal disease for all 15 patients was 33 Gy (range, 24–46 Gy), and the total doses of salvage cranial radiotherapy for 3 patients ranged from 18 Gy to 24 Gy (Table 4). These 3 patients had intracranial recurrences at lesions initially treated with doses of 20–24 Gy, and the recurrent diseases extended to the margins of initial boost radiation field. In the analysis, the presence of intracranial recurrence and salvage treatment modality (radiotherapy with chemotherapy vs. radiotherapy alone) had a statistically significant

Table 5. Univariate and multivariate analysis of various potential prognostic factors for spinal recurrence in patients with intracranial germinoma

Variable	No. of pts.	No. of spinal recurrence	Univariate	Multivariate	
			p value	RR (95%C1)	*p* value
Tumor size					
<4 cm	131	7 (5%)	< 0.001	0.141 (0.043–0.462)	0.001
≥4 cm	34	8 (24%)			
Tumor number					
Single	125	8 (6%)	0.033	0.230 (0.070–0.761)	0.016
Multifocal	40	7 (18%)			
Gender					
Female	38	5 (13%)	0.320	—	—
Male	127	10 (8%)			
Pathology					
Verified	102	11 (11%)	0.335	—	—
Unverified	63	4 (6%)			
Spinal MRI at diagnosis					
Yes	81	6 (7%)	0.460	—	—
No	84	9 (11%)			
Total radiation dose					
≤50 Gy	131	13 (10%)	0.470	—	—
>50 Gy	34	2 (6%)			
Serum hCG					
Normal	131	11 (8%)	0.542	—	—
High	34	4 (12%)			
KPS					
≥70%	128	13 (10%)	0.660	—	—
<70%	27	2 (7%)			
Unknown	10				
Radiation field					
WB/WV	145	13 (9%)	0.880	—	—
Local	20	2 (10%)			
Age					
<20 y	109	10 (9%)	0.897	—	—
≥20 y	56	5 (9%)			
Use of chemotherapy					
Yes	75	7 (9%)	0.920	—	—
No	90	8 (9%)			

Abbreviations: MRI = magnetic resonance imaging; hCG = human chorionic gonadtropin; KPS = Karnofsky performance status; WB/WV = whole brain/whole ventricle; RR = relative risk; CI = confidence intervals.

impact on DFS (Table 7). All 3 patients treated with spinal radiotherapy alone died of the disease and all 4 patients with intracranial recurrence died of the disease or were alive with the recurrent disease during the period of this analysis.

Concerning intracranial recurrence and treatment modality, we defined the favorable-prognosis group as patients with no intracranial recurrence who were treated with both spinal radiotherapy and chemotherapy, and the unfavorable-prognosis group as patients with intracranial recurrence or those treated with radiotherapy alone. Four of 9 patients from the favorable risk group and 3 of 6 patients from the unfavorable risk group had spinal MRI evaluation at the time of initial diagnosis. The 3-year DFS rate in the favorable prognosis group was 100%, but only 17% in unfavorable prognosis group ($p = 0.001$, Fig. 2). No patients in the favorable risk group developed late complications, such as neurocognitive dysfunctions, vascular pathology, or leukoencephalopathy after salvage treatments.

Table 6. Incidences of spinal recurrence according to the maximal tumor size

Maximal tumor size	No. of pts.	No. of pts. with spinal recurrence
<2 cm	35	1 (3%)
≤2 cm <4 cm	96	6 (6%)
≥4 cm	34	8 (24%)
Total	165	15 (9%)

DISCUSSION

The current study indicated that large intracranial disease and multifocal intracranial disease at initial diagnosis were independent risk factors for spinal recurrence in patients with intracranial germinoma with no evidence of spinal metastases at diagnosis. Concerning the primary tumor size, several reports have indicated that tumor size is an independent prognostic factor for these tumors (6, 29, 30). Shibamoto *et al.* indicated that a tumor size <3 cm was associated with a better prognosis in patients with intracranial germinoma

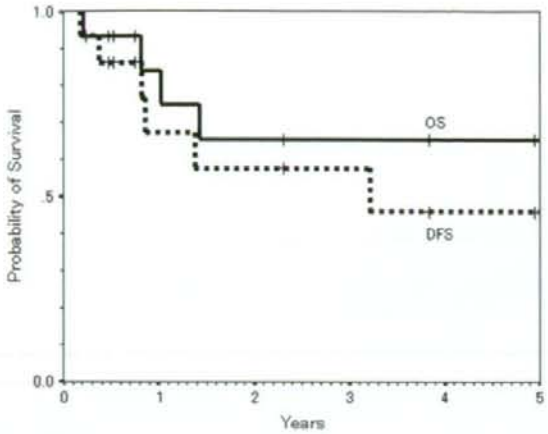

Fig. 1. Actuarial overall survival (OS) and disease-free survival (DFS) for all 15 patients with intracranial germinoma who developed spinal recurrence from the beginning of salvage treatment.

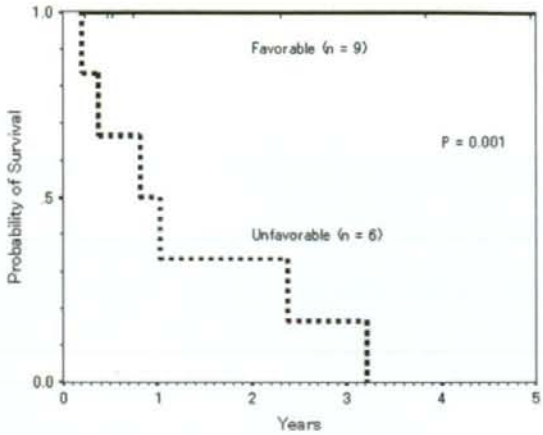

Fig. 2. Actuarial disease-free survival rates from the beginning of salvage treatment according to the presence of intracranial recurrence and treatment modality in patients with intracranial germinoma who developed spinal recurrences.

(30). Shirato *et al.* treated 51 patients with intracranial germinoma, and of 4 patients with more than 4-cm tumor, 1 patient (25%) had a spinal recurrence (6). In the current study, the incidence of spinal recurrence was significantly higher in patients with intracranially large tumor than those without large tumors, and large primary tumor was found to be an independent risk factor for spinal recurrence. These results suggest that craniospinal irradiation appears to be appropriate in patients with large primary tumors, even if there is no evidence of spinal metastases at diagnosis.

Table 7. Univariate analysis of various potential prognostic factors for disease-free survival in patients with intracranial germinoma who developed spinal recurrence

Variable	No. of pts.	3-year DFS (%)	*p* Value
Salvage treatment modality			
RT and CT	12	76	0.002
RT alone	3	0	
Presence of intracranial recurrence			
Yes	4	0	0.018
No	11	71	
Age			
<20 y	10	40	0.127
≥20 y	5	75	
Spinal radiation dose			
<40 Gy	9	38	0.163
≥40 Gy	6	75	
Pathology			
Verified	10	49	0.370
Unverified	5	67	
KPS			
≥70%	13	57	0.378
<70%	2	0	
Initial serum hCG level			
Normal	11	65	0.437
High	4	38	

Abbreviations: RT = radiotherapy; CT = chemotherapy; KPS = Karnofsky performance status; hCG = human chorionic gonadotropin; DFS = disease-free survival.

Concerning the number of primary tumors, several authors have recommended craniospinal irradiation for multifocal tumors (19, 31). Lindstadt *et al.* recommended that patients with documented subependymal or subarachnoid metastases presumably are at higher risk for leptomeningeal failure and recommended craniospinal irradiation for these patients (19). Dalttoli *et al.* advocated that craniospinal irradiation should be administered to patients with disease involving more than one intracranial site, demonstrated meningeal seeding, or positive cerebrospinal fluid cytology (31). In the current study, the incidence of spinal recurrence was significantly higher in patients with intracranially multifocal tumor at initial diagnosis than those without intracranially multifocal tumors. Moreover, the multivariate analysis revealed that multifocal primary tumor was found to be an independent risk factor for spinal recurrence. These results suggest that craniospinal irradiation appears to be appropriate in patients with multifocal tumors even if there is no evidence of spinal dissemination at the time of initial diagnosis.

However, optimal management of primary intracranial pineal and neurohypophyseal (bifocal) germinomas still remains controversial (3, 32, 33). Shibamoto *et al.* advocated that when the disease extends along the ventricular walls or is present in both pineal and neurohypophyseal regions, craniospinal irradiation should be considered, taking the patient's age into account (3). Conversely, Lafay-Cousin *et al.* suggested that bifocal germinoma can be considered a locoregional rather than a metastatic disease (33). The definition as either located or disseminated diseases has major implications on required treatment and its associated late morbidity. Moreover, the pathogenesis of such bifocal lesion is contested and the optimal management remains controversial. In the current study, 3 of 18 patients (17%) with bifocal germinoma had spinal recurrences. From our results, bifocal germinoma may

have some potential to metastasize and we advocate that patients with bifocal germinoma should be treated with craniospinal irradiation, taking the patient's age into account.

Although the optimal radiotherapy dose to the primary tumor is still unclear, recent findings have suggested that intracranial germinomas can be generally be cured with doses of between 40 and 50 Gy (3, 5, 6, 9, 20). In the current study, doses greater than 50 Gy were not associated with a decreased risk of spinal recurrence (Table 5). Therefore, doses of 40–50 Gy appear to be appropriate for the primary tumor. Concerning the optimal radiation dose required for the control of microscopic disease, most authors have recommended doses of 25–30 Gy for microscopic disease (7, 10, 13, 34). In the current study, we found that intracranial recurrences occurred with lesions treated at doses of 20–24 Gy in 3 patients, and that total doses of 24 Gy or less may be insufficient for microscopic diseases. Recently, Shibamoto *et al.* recommended a lower craniospinal dose of 20–24 Gy, because similar results were obtained for patient groups with positive or negative cytology (20). Schoenfeld *et al.* indicated that radiotherapy alone with low-dose prophylactic craniospinal irradiation (usually 21 Gy at 1.5 Gy per fraction) cured almost all patients with localized intracranial germinoma with rare complications (17). Further studies are needed to determine whether even lower doses can suffice for the control of microscopic disease.

Recently, to reduce the total radiation doses, the combination of chemotherapy and low-dose radiotherapy has being increasingly investigated (25, 26). The approach of delivering reduced-dose limited-field radiotherapy after a complete response to chemotherapy appears to be meritorious. However, our results indicated that chemotherapy was not associated with decreased risk of spinal recurrences (Table 5). Therefore chemotherapy alone appears to be insufficient to eradicate the microscopic spinal diseases, and spinal radiotherapy is recommended as a prophylactic treatment for spinal recurrence.

Concerning the treatment results for spinal recurrence, our results indicated that presence of intracranial recurrence and treatment modality (radiotherapy with chemotherapy vs. radiotherapy alone) each had a statistically significant impact on DFS. In particular, considering both the presence of intracranial recurrence and the treatment modality, the 3-year DFS in patients with no intracranial recurrence and treated with radiotherapy and chemotherapy was 100%, whereas only 17% in patients with intracranial recurrence and/or treated with radiotherapy alone ($p = 0.001$). Although there have been few reports describing the treatment results of spinal recurrences from intracranial germinoma, recent reports with unusual cases have indicated the efficacy of radiotherapy combined with chemotherapy for spinal tumors (35, 36). Merchant *et al.* treated 8 patients with intracranial germinoma who relapsed after treatment with primary chemotherapy. Of these 8 patients, 2 had spinal recurrences (tumor cells detected by MRI or cytologic evidence of cerebrospinal fluid involvement) and both were successfully treated with combination chemotherapy and radiotherapy (35). Tosaka *et al.* experienced a patient with spinal recurrence from intracranial germinoma who was successfully treated with 24 Gy spinal radiotherapy and several courses of systemic chemotherapy containing carboplatin, etoposide, and iphosphamide, with no recurrences after 1 year (36). Our results indicated that 3-year DFS in patients treated with radiotherapy and chemotherapy was significantly higher than that in patients treated with radiotherapy alone ($p = 0.002$). These results indicated that in patients with spinal recurrence alone, radiotherapy with chemotherapy was effective in controlling the recurrent diseases and should be recommended as a salvage treatment for these recurrent tumors.

Conversely, our results indicated that the patients with intracranial recurrences or treated with radiotherapy alone had a poor prognosis. For patients with intracranial recurrence, most patients have already received approximately 30–50 Gy to the brain and only insufficient radiation doses can be applied to the recurrent intracranial disease. In the current study, total doses of salvage cranial radiotherapy for 3 patients with intracranial recurrence were 18–24 Gy, which appeared to be insufficient for controlling the recurrent intracranial diseases, and all 3 patients were dead or alive with recurrent disease despite salvage therapies. Therefore, from our results, the optimal initial treatment at diagnosis is necessary to reduce the risk of intracranial recurrence (37–39). Concerning treatment modalities, our results indicated that 3 patients treated with spinal radiotherapy alone all died of the disease. Therefore spinal radiotherapy alone appears to be insufficient to control the recurrent spinal diseases.

In conclusion, our results indicated that large intracranial tumor and multifocal intracranial tumor were independent risk factors for spinal recurrence in patients with intracranial germinoma with no evidence of spinal metastases at initial diagnosis, and craniospinal irradiation appears to be appropriate for these patients. Our results also indicated that for patients who developed spinal recurrences alone, a combination of radiotherapy and chemotherapy was effective in controlling recurrent spinal diseases, and should be recommended as a salvage treatment for these recurrent tumors. However, this study is a retrospective study with a various treatment regimens, and further prospective studies are required to confirm our results.

REFERENCES

1. Bamberg M, Kortmann RD, Calaminus G, *et al.* Radiation therapy for intracranial germinoma: Results of the German cooperative prospective trials MAKEI 83/86/89. *J Clin Oncol* 1999;17: 2585–2592.
2. Sutton LN, Radcliffe J, Goldwein JW, *et al.* Quality of life of adult survivors of germinomas treated with craniospinal irradiation. *Neurosurgery* 1999;45:1292–1297.
3. Shibamoto Y, Abe M, Yamashita J, *et al.* Treatment results of intracranial germinoma as a function of the irradiated volume. *Int J Radiat Oncol Biol Phys* 1988;15: 285–290.
4. Aoyama H, Shirato H, Kakuto Y, *et al.* Pathologically-proven intracranial germinoma treated with radiation therapy. *Radiother Oncol* 1998;47:201–205.

5. Hardenbergh PH, Golden J, Billet A, *et al.* Intracranial germinoma: The case for lower dose radiation therapy. *Int J Radiat Oncol Biol Phys* 1997;39:419–426.
6. Shirato H, Nishio M, Sawamura Y, *et al.* Analysis of long-term treatment of intracranial germinoma. *Int J Radiat Oncol Biol Phys* 1997;37:511–515.
7. Brandes AA, Pasetto LM, Monfardini S. The treatment of cranial germ cell tumors. *Cancer Treat Rev* 2000;26:233–242.
8. Matsutani M, Sano K, Takakura K, *et al.* Primary intracranial germ cell tumors: A clinical analysis of 153 histologically verified cases. *J Neurosurg* 1997;86:446–455.
9. Shibamoto Y, Sasai K, Oya N, *et al.* Intracranial germinoma: Radiation therapy with tumor volume-based dose selection. *Radiology* 2001;218:452–456.
10. Haddock MG, Schild SE, Scheithauer BW, *et al.* Radiation therapy for histologically confirmed primary central nervous system germinoma. *Int J Radiat Oncol Biol Phys* 1997;38:915–923.
11. Ogawa K, Toita T, Nakamura K, *et al.* Treatment and prognosis of intracranial non-germinomatous malignant germ cell tumors: A multi-institutional retrospective analysis of 41 patients. *Cancer* 2003;98:369–376.
12. Paulino AC, Wen BC, Mohideen MN. Controversies in the management of intracranial germinomas. *Oncology (Williston Park)* 1999;13:513–521.
13. Fields JN, Fulling KH, Thomas PR, *et al.* Suprasellar germinoma: Radiation therapy. *Radiology* 1987;164:247–249.
14. Rogers SJ, Mosleh-Shirazi MA, Saran FH. Radiotherapy for localized intracranial germinoma: Time to sever historical ties? *Lancet Oncol* 2005;6:509–519.
15. Maity A, Shu HK, Janss A, *et al.* Craniospinal radiation in the treatment of biopsy-proven intracranial germinomas: Twenty-five years' experience in a single center. *Int J Radiat Oncol Biol Phys* 2004;58:1165–1170.
16. Merchant TE, Sherwood SH, Mulhern RK, *et al.* CNS germinoma: Disease control and long-term functional outcome for 12 children treated with craniospinal irradiation. *Int J Radiat Oncol Biol Phys* 2000;46:1171–1176.
17. Schoenfeld GO, Amdur RJ, Schmalfuss IM, *et al.* Low-dose prophylactic craniospinal radiotherapy for intracranial germinoma. *Int J Radiat Oncol Biol Phys* 2006;65:481–485.
18. Nguyen QN, Chang EL, Allen PK, *et al.* Focal and craniospinal irradiation for patients with intracranial germinoma and patterns of failure. *Cancer* 2006;107:2228–2236.
19. Linstadt D, Wara WM, Edwards MS, *et al.* Radiotherapy of primary intracranial germinomas: The case against routine craniospinal irradiation. *Int J Radiat Oncol Biol Phys* 1988;15: 291–297.
20. Ogawa K, Shikama N, Toita T, *et al.* Long-term radiotherapy for intracranial germinoma: A multi-institutional retrospective review of 126 patients. *Int J Radiat Oncol Biol Phys* 2004;58: 705–713.
21. Ogawa K, Toita T, Kakinohana Y, *et al.* Radiation therapy for intracranial germ cell tumors: Predictive value of tumor response as evaluated by computed tomography. *Int J Clin Oncol* 1997;2:67–72.
22. Shikama N, Ogawa K, Tanaka S, *et al.* Lack of benefit of spinal irradiation in the primary treatment of intracranial germinoma: A multiinstitutional, retrospective review of 180 patients. *Cancer* 2005;104:126–134.
23. Yoshida J, Sugita K, Kobayashi T, *et al.* Prognosis of intracranial germ cell tumours: Effectiveness of chemotherapy with cisplatin and etoposide (CDDP and VP-16). *Acta Neurochir (Wien)* 1993;120:111–117.
24. Matsutani M, Sano K, Takakura K, *et al.* Combined treatment with chemotherapy and radiation therapy for intracranial germ cell tumors. *Child Nerv Syst* 1998;14:59–62.
25. Aoyama H, Shirato H, Ikeda J, *et al.* Induction chemotherapy followed by low-dose involved-field radiotherapy for intracranial germ cell tumors. *J Clin Oncol* 2002;20:857–865.
26. Matsutani M. The Japanese Pediatric Brain Tumor Study Group. Combined chemotherapy and radiation therapy for CNS germ cell tumors—the Japanese experience. *J Neurooncol* 2001;54:311–316.
27. Kaplan EL, Meier P. Nonparametric estimation from incomplete observations. *J Am Stat Assoc* 1958;53:457–481.
28. Mantel N. Evaluation of survival data and two new rank order statistics arising in its consideration. *Cancer Chemother Rep* 1966;50:163–170.
29. Sung DI, Harisliadis L, Chang CH. Midline pineal tumors and suprasellar germinomas: Highly curable by irradiation. *Radiology* 1978;128:745–751.
30. Shibamoto Y, Yakahashi M, Abe M. Reduction of the radiation dose for intracranial germinoma: A prospective study. *Br J Cancer* 1994;70:984–989.
31. Dattoli MJ, Newall J. Radiation therapy for intracranial germinoma: The case for limited volume treatment. *Int J Radiat Oncol Biol Phys* 1990;19:429–433.
32. Lee L, Saran F, Hargrave D, *et al.* Germinoma with synchronous lesions in the pineal and suprasellar regions. *Child Nerv Syst* 2006;22:1513–1518.
33. Lafay-Cousin L, Millar BA, Mabbott D, *et al.* Limited-field radiation for bifocal germinoma. *Int J Radiat Oncol Biol Phys* 2006;65:486–492.
34. Packer RJ, Cohen BH, Cooney K. Intracranial germ cell tumors. *Ongologist* 2000;5:312–320.
35. Merchant TE, Davis BJ, Sheldon JM, *et al.* Radiation therapy for relapsed CNS germinoma after primary chemotherapy. *J Clin Oncol* 1998;16:204–209.
36. Tosaka M, Ogimi T, Itoh J, *et al.* Spinal epidural metastasis from pineal germinoma. *Acta Neurochir (Wien)* 2003;145: 407–410.
37. Osuka S, Tsuboi K, Takano S, *et al.* Long-term outcome of patients with intracranial germinoma. *J Neurooncol* 2007;83:71–79.
38. Nakamura H, Takeshima H, Makino K, *et al.* Recurrent intracranial germinoma outside the initial radiation field: A single-institution study. *Acta Oncol* 2006;45:476–483.
39. Shirato H, Aoyama H, Ikeda J, *et al.* Impact of margin for treatment volume in low-dose involved field radiotherapy after induction chemotherapy for intracranial germinoma. *Int J Radiat Oncol Biol Phys* 2004;60:214–217.

Radiat Med (2008) 26:343–347
DOI 10.1007/s11604-008-0238-7

ORIGINAL ARTICLE

Infectious mediastinitis after cardiovascular surgery: role of computed tomography

Tsuneo Yamashiro · Hisashi Kamiya
Sadayuki Murayama · Shinobu Unten
Tadashi Nakayama · Masaki Gibo · Yukio Kuniyoshi

Received: June 27, 2007 / Accepted: February 28, 2008

Abstract
Purpose. The aim of this study was to evaluate the effectiveness of computed tomography (CT) findings in the diagnosis of mediastinitis after cardiovascular surgery with median sternotomy.
Material and methods. A total of 122 patients were divided into two groups: the early group (≤21 days after surgery) and the late group (>21 days after surgery). Among them, six patients were ultimately diagnosed with infectious mediastinitis. CT findings in each patient were evaluated. Mediastinal fluid collections or free gas bubbles were regarded as the primary findings of mediastinitis.
Results. In the early group, sensitivity and specificity of the primary CT findings were 100% and 39%, respectively. In the late group, the sensitivity was 100% and the specificity 85%. Mediastinal fluid collections were observed in all six patients with mediastinitis.
Conclusion. Mediastinal fluid collections or free gas bubbles are not specific during the early postoperative period. However, after 21 days, these observations could be indicative of mediastinitis.

T. Yamashiro (✉) · H. Kamiya · S. Murayama · S. Unten · T. Nakayama · M. Gibo
Department of Radiology, Graduate School of Medical Science, University of the Ryukyus, 207 Uehara, Nishihara-cho, Okinawa 903-0215, Japan
Tel. +81-98-895-1162; FAX +81-98-895-1420
e-mail: clatsune@yahoo.co.jp

Y. Kuniyoshi
Thoracic and Cardiovascular Surgery, Department of Bioregulatory Medicine, Faculty of Medicine, University of the Ryukyus, Okinawa, Japan

Key words Mediastinitis · Median sternotomy · Cardiovascular surgery · Computed tomography

Introduction

Infectious mediastinitis is a serious complication following median sternotomy during cardiovascular surgery. Although the incidence is reported at 0.4%–5.0%, mortality is quite high, ranging from 12% to 50%, depending on the extent of the infection.[1–11]

Previous computed tomography (CT) analyses in the setting of mediastinitis[1–8,12,13] have suggested that the primary hallmarks of mediastinitis include mediastinal fluid collections and/or free gas bubbles. However, the same findings have been made in normal patients after cardiovascular surgery, particularly during the early postsurgical period. It has been reported that these findings in normal patients may be present 2–3 weeks after sternotomy,[3,7,13] however, a few authors have noted that the number of postoperative days is significant for CT diagnosis of mediastinitis.[4,6] Given the seriousness of the disease, it is important to clarify the postsurgical CT findings.

We describe the effectiveness of CT scans in the diagnosis of mediastinitis, emphasizing the importance of the clinical time course. This report supplements two other previous studies of CT specificity in the postoperative setting.[4,6] Limitations in the use of contrast media are also discussed.

Materials and methods

From January 2005 to December 2006, a total of 111 consecutive patients were identified who underwent

thoracic CT within 90 days of cardiovascular surgery with median sternotomy. A retrospective study was undertaken using medical records and CT scans. This study was exempted from the approval of the institutional review board in our institution. One patient was excluded from the study because of the extremely poor quality of the CT images. To simplify the study model, another five patients who were diagnosed with osteomyelitis or deep wound infection were excluded from the study. Previous reports suggested that usually postoperative changes may persist for 3 weeks.[3,7,13] For that reason, we classified the patients on the basis of the number of postoperative days, within or after 21 days of surgery. Altogether, 17 patients who were not diagnosed with mediastinitis were scanned twice within and after 21 days.

Finally, 122 patients were divided into two groups. The early group included 71 patients who were examined within 21 days of surgery (range 2–21 days, mean 13 days). There were 47 males and 24 females with a median age of 65 years (range 16–83 years). The late group included 51 patients who were examined at least 21 days after surgery (range 22–87 days, mean 37 days). There were 32 males and 19 females with a median age of 66 years (range 31–88 years). In each group, CT scans were performed to check for mediastinitis or to observe the results of an aortic graft.

Six patients developed infectious mediastinitis, which was diagnosed by cardiovascular surgeons. Two patients were in the early group and four in the late group. Each patient's decisive CT scan was selected for the study, and all follow-up scans were excluded. Documentation of the diagnoses was based on positive bacterial cultures from (1) mediastinal pus and/or fluid collections obtained during a redo operation or (2) percutaneous drainage and/or discharge of midline wounds. Mediastinitis was caused by methicillin-resistant *Staphylococcus aureus* (MRSA) in five patients and methicillin-sensitive *Staphylococcus aureus* (MSSA) in the sixth patient. Despite a redo operation, one patient died of septic shock and multiple organ failure 4 days after the CT scan. The other five patients—treated by redo operation, percutaneous drainage, and antibiotics—recovered successfully.

Computed tomography was performed with a helical technique (LightSpeed QX/i, GE Medical Systems, Milwaukee, WI, USA; or X-vigor, Toshiba, Tokyo, Japan), including a series with a section thickness of 5.0 or 7.5 mm/15 mm table feed (pitch 0.75) on the GE instrument and a series with a section thickness of 5.0 mm/7 mm table feed (pitch 1.4) or 10 mm/10 mm (pitch 1) on the Toshiba device. The scanning time for each section was ≤1.0 s. The matrix size was 512 × 512 pixels.

Altogether, 32 patients in the early group and 40 patients in the late group received 100 ml of intravenous nonionic contrast medium. The injection rates were 2 ml/s or 3 ml/s (scan delays were 45 or 30 s, respectively). Obtained images, 5.0 or 7.5 mm (GE) and 5 mm or 10 mm (Toshiba) in thickness, were shown at appropriate mediastinal and bone window width and levels (350 HU/40 and 1500 HU/600).

Imaging evaluations were performed independently on monitor viewing by two board-certified radiologists (T.Y., H.K.). Each CT scan was reviewed randomly without clinical information or the final diagnosis. Reviewers separately evaluated the presence of CT findings that are mentioned below. Discordant results were discussed and assessed by consensus.

The CT findings were categorized as follows: localized mediastinal fluid collections, free gas bubbles in the mediastinum, increased attenuation of mediastinal fat, lymphadenopathy (>10 mm in the short axis), pericardial effusion, pleural effusion, and sternal abnormality. Sternal abnormalities were divided into dehiscence (>5 mm), destruction, and presternal fluid collections. According to previous reports, localized mediastinal fluid collections or free gas bubbles were regarded as the primary CT findings that indicated mediastinitis.[4,6] Sensitivity and specificity of these primary findings were evaluated in each group.

Results

Table 1 gives the CT findings for each patient group. In the early group (Figs. 1, 2), CT scans revealed localized mediastinal fluid collections in 32 of 71 patients. Free gas bubbles were seen in 28 patients, increased attenuation of mediastinal fat in 48 patients, and lymphade-

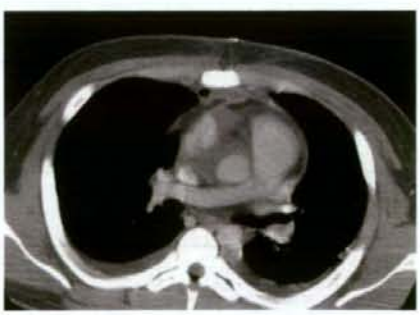

Fig. 1. True-positive case in the early group: [methicillin-resistant *Staphylococcus aureus* (MRSA) infection]. A 16-year-old boy 8 days after aortic valve replacement. Note the free gas bubble and retrosternal fluid collections with contrast enhancement as well as pericardial effusions and bilateral pleural effusions

Table 1. CT features in each patient group

CT findings	Early group ($n = 71$)	Late group ($n = 51$)
Mediastinal fluid collection	32 (45%)	10 (20%)
Free gas bubbles	28 (39%)	5 (10%)
Increased attenuation of mediastinal fat	48 (68%)	23 (45%)
Lymphadenopathy	6 (8%)	9 (18%)
Pericardial effusion	38 (54%)	19 (37%)
Pleural effusion	58 (82%)	30 (59%)
Sternal dehiscence	0	2 (4%)
Sternal destruction	0	1 (2%)
Presternal fluid collection	3 (4%)	3 (6%)

CT, computed tomography

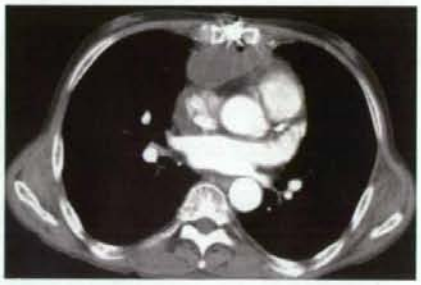

Fig. 2. False-positive case in the early group. A 66-year-old man 11 days following mitral valve plasty. Note the gas bubble and large fluid collection in the anterior mediastinum with contrast enhancement of the margin

Fig. 3. True-positive case in the late group (MRSA infection). A 53-year-old man 48 days after coronary artery bypass grafting. Note the mediastinal fluid collection without obvious contrast enhancement and increased attenuation of mediastinal fat

nopathy in 6 patients. Pericardial effusions were revealed in 38 patients and pleural effusions in 58 patients (bilateral in 35 and unilateral in 23). Among sternal abnormalities, presternal fluid collections were observed in three patients. Neither dehiscence nor destruction was observed. In this group, only two patients were ultimately diagnosed with infectious mediastinitis. Both demonstrated mediastinal fluid collections with contrast enhancement, free gas bubbles, increased attenuation of mediastinal fat, and bilateral pleural effusions.

In the late group (Figs. 3, 4), localized mediastinal fluid collections were observed in 10 of 51 patients. Free gas bubbles were seen in 5 patients, increased attenuation of mediastinal fat in 23 patients, lymphadenopathy in 9 patients, pericardial effusions in 19 patients, and pleural effusions in 30 patients (bilateral in 12 and unilateral in 18). Sternal dehiscence was observed in two patients, sternal destruction in one, and presternal fluid collections in three. In this group, four patients were eventually diagnosed with mediastinitis. All four had mediastinal fluid collections and increased attenuation of mediastinal fat. Three of them demonstrated free gas bubbles, pericardial effusions, and presternal fluid collections. Bilateral pleural effusions were observed in two

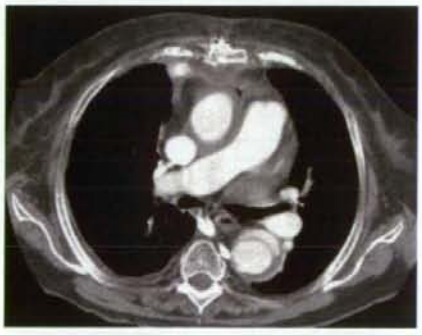

Fig. 4. False-positive case in the late group. An 85-year-old woman 25 days after graft replacement of the ascending aorta. There is a retrosternal fluid collection and a gas bubble

of the four patients. One patient with mediastinitis did not show obvious contrast enhancement at the rims of the mediastinal fluid collections.

When localized mediastinal fluid collections or free gas bubbles were defined as the CT criteria for diagnosing mediastinitis, results of the two groups were as follows (Table 2). In the early group, there were 2 true-

Table 2. Sensitivity and specificity of the primary CT findings

Groups	True (+)	True (−)	False (+)	False (−)	No. of patients	Sensitivity (%)	Specificity (%)
Early	2	27	42	0	71	100	39
Late	4	40	7	0	51	100	85

positive, 27 true-negative, 42 false-positive, and no false-negative CT examinations. In the late group, there were 4 true-positive, 40 true-negative, 7 false-positive, and no false-negative examinations. All patients with false-positive CT examinations had been examined within 35 days of surgery. Thus, the sensitivity and specificity of CT diagnoses in the early group (≤21 days after surgery) were 100% and 39%, respectively; and in the late group (>21 days after surgery), the sensitivity was 100% and the specificity 85%.

Among the early group patients with false-positive CT results, 14 had both mediastinal fluid collections and free gas bubbles, 13 also showed mediastinal fluid collections with bilateral pleural effusions, and 7 demonstrated strong enhancement at the rims of mediastinal fluid collections. Among the late group patients with false-positive CT results, one had mediastinal fluid collections and free gas bubbles, three had mediastinal fluid collections with bilateral pleural effusions, and four showed strong enhancement at the rims of mediastinal fluid collections.

Discussion

Among CT findings of infectious mediastinitis, localized mediastinal fluid collection and/or free gas bubbles are thought to be its primary findings.[4,6] However, during the early period following sternotomy, these findings are not reliable indicators of infectious mediastinitis because they are detected in a high proportion of patients.[2–8,13] For example, these findings may be present 2–3 weeks after sternotomy in normal postoperative patients.[3,7,13] As a result, some investigators have concluded that CT has limited usefulness in the diagnosis of postsurgical mediastinitis.[5,8] Others emphasize the importance of the clinical time course and suggest that these findings are highly indicative of mediastinitis after postoperative day 14[6] or after day 17.[4]

Free gas bubbles in the mediastinum are important in the diagnosis of mediastinitis due to esophageal perforation or acute descending necrotizing mediastinitis.[4] However, they are frequently observed during the early poststernotomy period.[3,4,6,13] It has been suggested that bubbles in the mediastinum might be normal for 7–20 days following surgery[7,13] In our study, free gas bubbles were demonstrated frequently as a false-positive finding in the early group. Additionally, one patient without mediastinitis in the late group showed gas bubbles 25 days after surgery. Thus, we propose that free gas bubbles in the mediastinum are common and so are not valuable, particularly during the early postsurgical period.

Detection of localized mediastinal fluid collection is also ambiguous. Although it may indicate mediastinitis when sustained after postoperative day 14,[6] it has been reported that in only one of five patients who showed retrosternal fluid collection more than 30 days after surgery was it representative of mediastinitis.[8] In our study, six asymptomatic patients in the late group (examined 22–35 days after surgery) demonstrated localized mediastinal fluid collections. Thus, these collections may persist for up to 35 days after surgery.

It has also been suggested that if a mediastinal soft tissue mass (fluid collection) is found in combination with bilateral pleural effusion, the possibility of mediastinitis is much higher than if either is found separately.[2] In our study, four of six patients who were diagnosed for mediastinitis showed these findings. However, 16 patients without mediastinitis (13 in the early group, 3 in the late group) also had them. We suggest that localized mediastinal fluid collection with bilateral pleural effusion is not a definitive finding for mediastinitis.

From the perspective of the clinical time course, our results suggest that localized mediastinal fluid collections or free gas bubbles are indicative of mediastinitis 21 days after surgery with a specificity of 85%. This result demonstrates lower reliability than others have reported.[4,6,7] We emphasize that, in our study, the false-positive cases occurred even after 21 days of surgery. This fact underscores the difficulty of arriving at an accurate radiological diagnosis and the importance of other clinical or laboratory findings. Note also that many cases of postoperative mediastinitis occur within 2 weeks of surgery,[5,9–11] at which time radiological diagnosis would be of limited value. With a CT-based diagnosis of postoperative mediastinitis, therefore, radiologists must be aware of the importance of the clinical time course and limitations, particularly during the early postsurgical period.

Although the effectiveness of contrast media in the diagnosis of mediastinitis has received little interest, it has been reported that infected mediastinal fluid collec-

tions do not always demonstrate contrast enhancement.[4] The same tendency was observed in the present study. Furthermore, noninfectious mediastinal fluid collection was occasionally enhanced in the false-positive patients. Given these results, we are skeptical about the reliability of contrast enhancement during the postsurgical period.

Limitations of our study include reliance on a retrospective approach and the small number of patients, in particular, those with mediastinitis. We could not estimate the accuracy of the primary CT findings of mediastinitis. Because we excluded patients with osteomyelitis or deep wound infection to simplify the study model, we did not resolve the similarities and disparities of CT findings between mediastinitis and osteomyelitis. In addition, CT was not always performed for poststernotomy patients at our institution because many of them recovered uneventfully or their grafts were examined by conventional angiography. Furthermore, contrast medium was not always given, particularly in the early group, because of each patient's condition. Further evaluation is recommended to evaluate the true reliability of the primary findings and the contrast enhancement of mediastinal fluid collection.

Conclusion

Our results have identified two primary CT findings that predict mediastinitis with high specificity after 21 days of surgery: localized mediastinal fluid collections and free gas bubbles in the mediastinum. However, physicians must take into consideration the postsurgical course and the importance of other clinical information to make a correct diagnosis. Contrast enhancement of mediastinal fluid collections must be evaluated carefully as enhancement may be observed in noninfectious fluid collections.

References

1. Carrol CL, Jeffrey RB, Federle MP, Vernacchia FS. CT evaluation of mediastinal infections. J Comput Assist Tomogr 1987;11:449–54.
2. Misawa Y, Fuse K, Hasegawa T. Infectious mediastinitis after cardiac operations: computed tomographic findings. Ann Thorac Surg 1998;65:622–4.
3. Templeton PA, Fishman EK. CT evaluation of poststernotomy complications. AJR Am J Roentgenol 1992;159:45–50.
4. Exarhos DN, Malagari K, Tsatalou EG, Benakis SV, Peppas C, Kotanidou A, et al. Acute mediastinitis: spectrum of computed tomography findings. Eur Radiol 2005;15:1569–74.
5. Yamaguchi H, Yamauchi H, Yamada T, Ariyoshi T, Aikawa H, Kato Y. Diagnostic validity of computed tomography for mediastinitis after cardiac surgery. Ann Thorac Cardiovasc Surg 2001;7:94–8.
6. Jolles H, Henry DA, Roberson JP, Cole TJ, Spratt JA. Mediastinitis following median sternotomy: CT findings. Radiology 1996;201:463–6.
7. Goodman LR, Kay HR, Teplick SK, Mundth ED. Complications of median sternotomy: computed tomographic evaluation. AJR Am J Roentgenol 1983;141:225–30.
8. Bitkover CY, Cederlund K, Aberg B, Vaage J. Computed tomography of the sternum and mediastinum after median sternotomy. Ann Thorac Surg 1999;68:858–63.
9. Trouillet JL, Vuagnat A, Combes A, Bors V, Chastre J, Gandjbakhch I, et al. Acute poststernotomy mediastinitis managed with debridement and closed-drainage aspiration: factors associated with death in the intensive care unit. J Thorac Cardiovasc Surg 2005;129:518–24.
10. Loop FD, Lytle BW, Cosgrove DM, Mahfood S, McHenry MC, Goormastic M, et al. Sternal wound complications after isolated coronary artery bypass grafting: early and late mortality, morbidity, and cost of care. Ann Thorac Surg 1990;49:179–87.
11. Bitkover CY, Gardlund B. Mediastinitis after cardiovascular operations: a case-control study of risk factors. Ann Thorac Surg 1998;65:36–40.
12. Breatnach E, Nath PH, Delany DJ. The role of computed tomography in acute and subacute mediastinitis. Clin Radiol 1986;37:139–45.
13. Kay HR, Goodman LR, Teplick SK, Mundth ED. Use of computed tomography to assess mediastinal complications after median sternotomy. Ann Thorac Surg 1983;36:706–14.

Cardiovasc Intervent Radiol (2008) 31:91–97
DOI 10.1007/s00270-007-9170-y

CLINICAL INVESTIGATION

Impact of Multislice CT Angiography on Planning of Radiological Catheter Placement for Hepatic Arterial Infusion Chemotherapy

Miyuki Sone · Kenichi Kato · Atsuo Hirose · Tatsuhiko Nakasato · Makiko Tomabechi · Shigeru Ehara · Takao Hanari

Received: 30 December 2006 / Accepted: 10 September 2007 / Published online: 10 October 2007

Abstract The objective of this study was to assess prospectively the role of multislice CT angiography (MSCTA) on planning of radiological catheter placement for hepatic arterial infusion chemotherapy (HAIC). Forty-six patients with malignant liver tumors planned for HAIC were included. In each patient, both MSCTA and intra-arterial digital subtraction angiography (DSA) were performed, except one patient who did not undergo DSA. Comparison of MSCTA and DSA images was performed for the remaining 45 patients. Detectability of anatomical variants of the hepatic artery, course of the celiac trunk, visualization scores of arterial branches and interobserver agreement, presence of arterial stenosis, and technical outcome were evaluated. Anatomical variations of the hepatic artery were detected in 19 of 45 patients (42%) on both modalities. The course of the celiac trunk was different in 12 patients. The visualization scores of celiac arterial branches on MSCTA/DSA were 3.0 ± 0/2.9 ± 0.2 in the celiac trunk, 3.0 ± 0/2.9 ± 0.3 in the common hepatic artery, 2.9 ± 0.2/2.9 ± 0.3 in the proper hepatic artery, 2.9 ± 0.3/2.9 ± 0.4 in the right hepatic artery, 2.8 ± 0.4/2.9 ± 0.4 in the left hepatic artery, 2.9 ± 0.2/2.9 ± 0.3 in the gastroduodenal artery, 2.1 ± 0.8/2.2 ± 0.9 in the right gastric artery, and 2.7 ± 0.8/2.6 ± 0.8 in the left gastric artery. No statistically significant differences exist between the two modalities. Interobserver agreement for MSCTA was equivalent to that for DSA. Two patients showed stenosis of the celiac trunk on both modalities. Based on these imaging findings, technical success was accomplished in all patients. In conclusion, MSCTA is accurate in assessing arterial anatomy and abnormalities. MSCTA can provide adequate information for planning of radiological catheter placement for HAIC.

Keywords Liver cancer · Hepatic arterial infusion chemotherapy · Multislice CT · CT angiography

M. Sone (✉) · K. Kato · T. Nakasato · M. Tomabechi · S. Ehara
Department of Radiology, Iwate Medical University, 19-1, Uchimaru, Morioka 0208505, Japan
e-mail: msone@athena.ocn.ne.jp

A. Hirose
Department of Radiology, Morioka Red-Cross Hospital, 6-1-1, Sanbonyanagi, Morioka 0208560, Japan

T. Hanari
Center for Radiological Sciences, Iwate Medical University, 19-1, Uchimaru, Morioka 0208505, Japan

Introduction

Hepatic arterial infusion chemotherapy (HAIC) is an established treatment for unresectable malignant hepatic neoplasm [1–3]. Although a few randomized control trials have shown a survival benefit of HAIC [4, 5], HAIC still remains an important treatment option because of the higher response rate and lower systemic toxicities compared with systemic chemotherapy [1–5]. For the implantation of a catheter and port system, a percutaneous approach using techniques of interventional radiology is now widely used instead of surgical methods [1, 3]. Radiological catheter placement consists of serial procedures including unification of multiple hepatic arteries, embolization of gastrointestinal branches arising from the hepatic artery, and implantation of a catheter and port system. All these procedures are needed to accomplish the adequate distribution of anticancer agents to the entire liver without extrahepatic perfusion through the implanted

catheter and port system [1, 3, 6]. Incorrect evaluation of vascular anatomy sometimes leads to inadequate situations such as a defect of drug distribution in the liver, gastrointestinal complication, or catheter-related arterial occlusion resulting in treatment failure. Thus, vascular mapping is essential for planning of radiological catheter placement. Although conventional angiography has been used for such assessment, multislice CT angiography (MSCTA) may be suitable for noninvasive abdominal vascular evaluation [7–10]. However, the specific need for radiological catheter and port placement by interventional radiologists, such as variations of the hepatic artery, gastrointestinal branches arising from hepatic arteries, and the course of the celiac trunk, has not been well evaluated. The purpose of this study was to assess prospectively the role of MSCTA in planning of radiological catheter placement for HAIC.

Materials and Methods

Patients

Between August 2003 and March 2007, eligible patients were enrolled in this study. Eligibility criteria were as follows: (a) patients planned to undergo radiological catheter and port placement for HAIC, (b) patients without prior catheter placement for HAIC or any kind of embolotherapy to the celiac or hepatic arterial region, (c) patients without a history of adverse reaction to contrast material and renal dysfunction (serum creatinine ≥ 2.0), and (d) written informed consent obtained. This study protocol was approved by the institutional review board of our institution.

MSCT Image Acquisition and Postprocessing

A 16-channel multislice CT scanner (Aquilion-16; Toshiba Medical Systems, Tokyo) was used for the evaluation. MSCTA was performed as part of a pretreatment routine CT evaluation of the abdomen. Ninety to one hundred milliliters of nonionic contrast material (iohexol; Omnipaque 300 syringe; Daiichi-Sankyo, Inc., Tokyo) was administered into the antecubital vein at a rate of 3 mL/s with an automated injector (Dual Shot/ A-300; Nemoto Kyorindo, Tokyo). For MSCTA, arterial-phase image scanning was started within 8 s after reaching the bolus of contrast material into the descending aorta (100 HU), using a bolus-tracking method. Images were obtained during inspiration. A collimation of 0.5 mm with a helical pitch of 15 was used. Three-dimensional (3-D) reconstruction was obtained on a dedicated workstation (Zio M900; Amin, Tokyo). For 3-D image reconstruction, multiplanar volume reformation (MPVR) images were obtained. When small vessels, including the right gastric artery, were not visualized on conventional MPVR images, additional images using targeted MPVR technique were used.

Digital Subtraction Angiography

Intra-arterial digital subtraction angiography (DSA) using Seldinger's technique was performed just before implantation of the catheter and port system, within 2 weeks after MSCTA. A transfemoral 5-Fr simple curved catheter was inserted selectively into the celiac trunk. Twenty to twenty-five milliliters of nonionic contrast material (iopamidol; Iopamiron 300; Bayer-Schering Pharma, Tokyo) was administered at a rate of 4–5 mL/s. Images were obtained during expiration.

Image Interpretation and Evaluation

Four radiologists evaluated MSCTA and DSA images independently, blinded to the other observers' results or patient history. A 4-week interval was set between the sessions for evaluation of two modalities to eliminate the awareness of the findings of another modality. Arterial anatomy and abnormalities were assessed regarding the following items.

1. Anatomic variation of the hepatic artery
2. Course of the celiac trunk: cranial, horizontal, or caudal
3. Visualization of the following vessels: celiac trunk, common hepatic artery (CHA), proper hepatic artery (PHA), right hepatic artery (RHA), left hepatic artery (LHA), gastroduodenal artery (GDA), right gastric artery (RGA), and left gastric artery (LGA). Visualization scores were on a scale of 1–3 (1, not visualized; 2, fair visualization [i.e., only origin or proximal portion of the artery recognizable]; 3, excellent visualization (i.e., entire course of the artery recognizable). Interobserver agreement was also evaluated.
4. Stenosis of ≥50% in any segment of the hepatic arteries

Estimation of Radiation Dose

Radiation exposure was estimated by measuring the volume computed tomography dose index (CTDIvol) and dose length product (DLP). CTDIw (mGy) was automatically calculated and displayed on the CT scanner using particular

parameters for the specific imaging protocol mentioned above. DLP (mGy · cm) was calculated by the following formula [11]:

$$DLP = CTDIvol \cdot \text{scan length}$$

where scan length (cm) is the length of the scan for individual patients.

Technical Outcome

Technical success was evaluated regarding unification of multiple hepatic arteries, embolization of gastric arteries, and implantation of catheter and port system.

Statistical Analysis

Sensitivity and specificity were calculated for each arterial segment. Visualization scores between MSCTA and DSA were compared by two-sided Wilcoxon's signed-rank test. The interobserver agreement for visualization score of MSCTA and DSA was evaluated using the κ value of two readers among four (six pairs each). Perfect agreement resulted in a κ value of 1; agreement expected on the basis of chance alone resulted in a κ value of 0. All calculations were performed using statistical analysis software (Dr. SPSS II 11.0.1J; SPSS Inc., Chicago, IL).

Results

Patient Characteristics

Forty-six patients with unresectable malignant liver tumors, 29 males and 17 females, ranging in age from 36 to 83 years (median, 63 years), were enrolled in this study. Thirty-three patients had metastatic liver tumors, seven had hepatocellular carcinoma, three had gallbladder carcinoma, and three had cholangiocellular carcinoma.

Image Evaluation

In all patients, MSCTA examination was technically adequate and was suitable for analysis. In one patient, DSA was not performed, because MSCTA showed severe stenosis of the common celiac trunk and the superior mesenteric artery (i.e., celiacomesenteric trunk), and we judged that insertion of an angiographic catheter for DSA and placement of an arterial infusion catheter should be avoided to prevent catheter-related complications such as vascular injury and spasm resulting in possible hepatic or mesenteric ischemia, due to this anatomical variation. Therefore, 45 of 46 patients underwent DSA and entered in the analysis.

Table 1 Anatomic variations in hepatic artery on MSCTA and DSA (number of arteries)

	MSCTA	DSA
Total	19	19
RHA from SMA	12	12
LHA from LGA	6	6
RHA from CHA	1	1

Note. MSCTA, multislice CT angiography; DSA, digital subtraction angiography; RHA, right hepatic artery; SMA, superior mesenteric artery; LHA, left hepatic artery; LGA, left gastric artery; CHA, common hepatic artery

Anatomical variations of the hepatic artery were present in 19 of 45 patients (42%) on both MSCTA and DSA (Table 1, Figs. 1 and 2). The sensitivity of MSCTA was 100% and the specificity was 100% when DSA was used as the gold standard. On MSCTA and DSA, the course of the proximal portion of the celiac trunk was cranial in 9 patients on MSCTA/13 patients on DSA, horizontal in 7 on MSCTA/9 on DSA, and caudal in 29 on MSCTA and 23 on DSA. So, the courses of the celiac trunk in two modalities were not corresponding in 12 patients. Regarding the visualization scores of each arterial segment, no statistically significant differences were noted between MSCTA and DSA (Table 2, Figs. 3 and 4). κ values, which were used to assess interobserver agreement for visualization scores, ranged from 0.47 to 0.50 (mean, 0.49) for MSCTA and from 0.41 to 0.57 (mean, 0.48) for DSA. Stenosis of the celiac trunk was noted in two patients on both MSCTA and DSA (Fig. 5).

Technical Outcome

Except for one patient who did not undergo DSA and catheter placement due to MSCTA findings mentioned above, 45 patients in this study received interventional procedures—unification of multiple hepatic arteries, embolization of gastric arteries arising from hepatic arteries, and catheter placement—which were successful in all patients.

Estimated Radiation Dose

Calculated CTDIvol for this MSCTA acquisition protocol was 33.8 mGy. Mean DLP ± standard deviation was 773 ± 95 mGy.

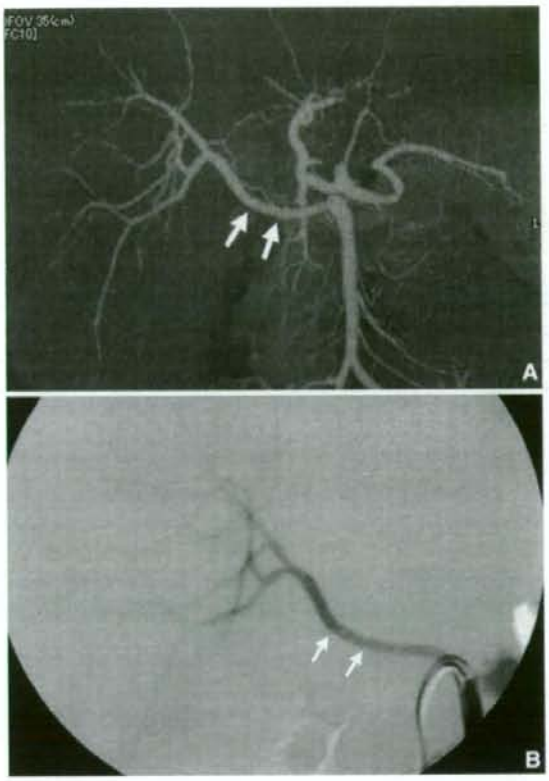

Fig. 1 Replaced right hepatic artery in a 46-year-old man with liver metastases. **A** MSCTA shows the right hepatic artery originating from the superior mesenteric artery (SMA; arrows). **B** Digital subtraction angiogram (DSA) of the SMA confirms the CT findings

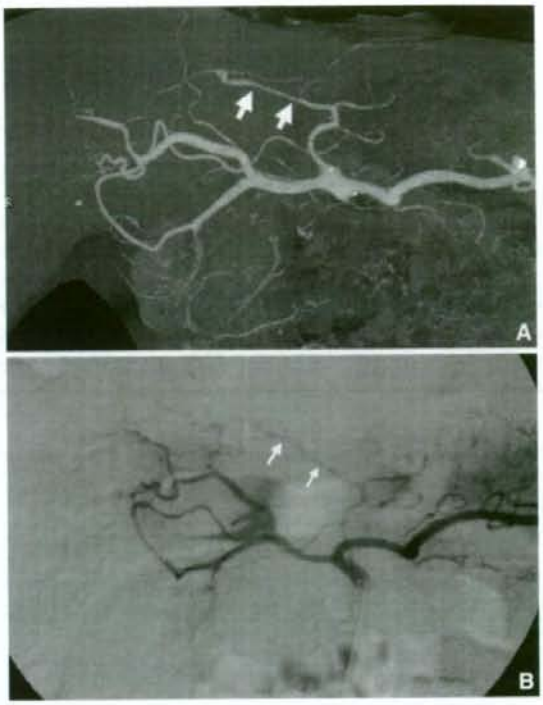

Fig. 2 Replaced left hepatic artery in a 73-year-old man with liver metastases. **A** MSCTA shows the left hepatic artery originating from the left gastric artery (arrows). **B** DSA of the celiac trunk confirms the CT findings

Table 2 Visualization scores for each arterial segment

	MSCTA	DSA	*p*
Celiac trunk	3.0 ± 0	2.9 ± 0.2	0.080
CHA	3.0 ± 0	2.9 ± 0.3	0.220
PHA	2.9 ± 0.2	2.9 ± 0.3	0.079
RHA	2.9 ± 0.3	2.9 ± 0.4	0.371
LHA	2.8 ± 0.4	2.9 ± 0.4	0.392
GDA	2.9 ± 0.2	2.9 ± 0.3	0.076
RGA	2.1 ± 0.8	2.2 ± 0.9	0.318
LGA	2.7 ± 0.8	2.6 ± 0.8	0.236

Note. Score: 1, not visualized; 2, fair; 3, excellent. CHA, common hepatic artery; PHA, proper hepatic artery; RHA, right hepatic artery; LHA, left hepatic artery; GDA, gastroduodenal artery; RGA, right gastric artery; LGA, left gastric artery

Discussion

This prospective study shows that MSCTA provides important information for radiological catheter and port placement for HAIC. Anatomical variation of the hepatic artery was demonstrated in 50% of patients on MSCTA, with a sensitivity of 100% and a specificity of 100%. Visualization of each vascular segment showed no statistically significant differences between MSCTA and DSA. Interobserver agreement for visualization score of MSCTA was equivalent to that of DSA.

The hepatic vessels have a complicated anatomy, and we frequently face anatomical variants during the interventional procedure of hepatic arterial catheter placement. Such variants of the hepatic artery affect the technical outcome of our interventional procedure. If there are any replaced or accessory hepatic arteries, arterial redistribution to unify hepatic arteries is required to achieve the delivery of chemotherapeutic agents to the entire liver via an indwelling catheter [1, 3]. Recent studies have shown that MSCTA is accurate in assessing hepatic and gastric arteries [7–10]. The improvement in longitudinal resolution with MSCT is a substantial advantage over single helical or nonhelical CT [7–13]. The shorter acquisition time may also be advantageous for obtaining a pure arterial phase by eliminating contamination of venous or

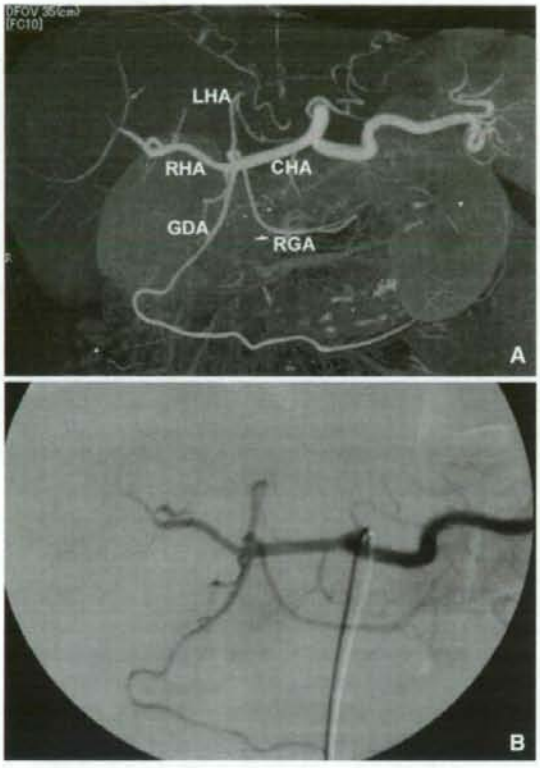

Fig. 3 A 79-year-old man with liver metastases. **A** MSCTA shows the hepatic and gastrointestinal branches of the hepatic arteries. **B** DSA confirms the CT findings

portal venous structures [13–14]. In previous studies, MSCTA demonstrated anatomical variation in 35% to 69% of patients [8, 9, 12, 14]. With regard to preoperative evaluation for surgical HAIC pump placement using laparotomy, two studies demonstrated an advantage of MSCTA [15, 16]. However, there is no report on CTA regarding radiological catheter and port placement. In radiological catheter and port placement, gastrointestinal arteries arising from hepatic arteries need to be embolized to avoid possible adverse gastrointestinal events due to exposure to high-dose chemotherapeutic agents [1, 3, 17]. Among the branches, the right gastric artery, arising from hepatic arteries, is relatively difficult to visualize on CTA because it tends to be small in diameter [10, 17]. Takahashi et al. reported the usefulness of MSCTA for depiction of small hepatic artery branches [10]. They reported that MSCTA detected 50 RGAs in 56 patients. The previous studies of preoperative assessment for HAIC pump under laparotomy did not include assessment of the gastroduodenal branches [15, 16]. In our study, mean visualization scores on MSCTA/DSA were 2.9 ± 0.2/

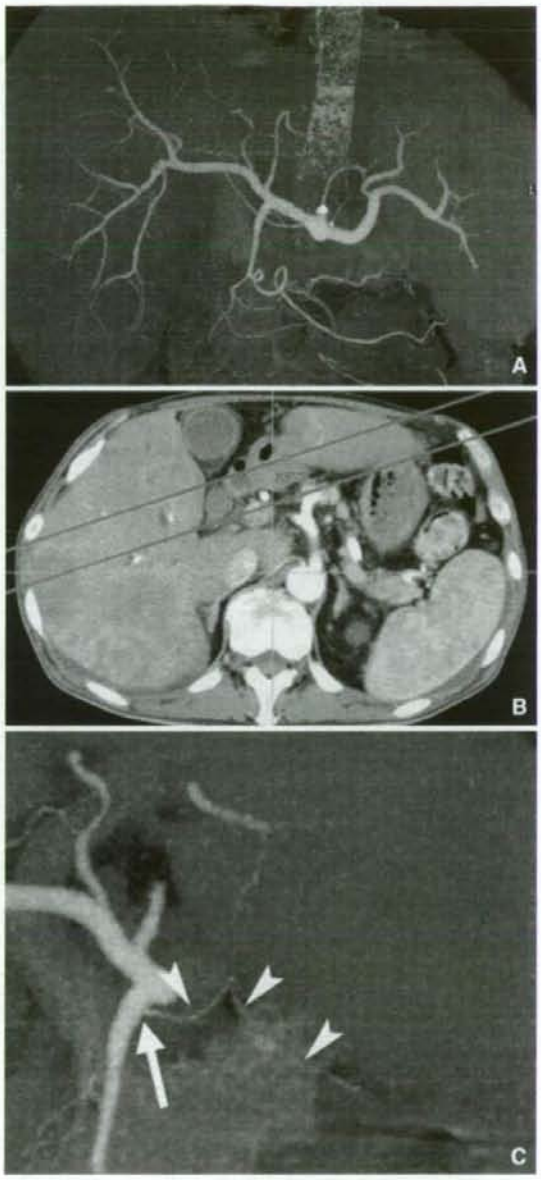

Fig. 4 A 75-year-old man with liver metastases. **A** MSCTA shows the right gastric artery (RGA), however, its origin is not clear. **B**, **C** MPVR image, targeted to the interval shown in B, demonstrates the origin (arrow) of the RGA (arrowheads)

2.9 ± 0.3 for GDA and 2.1 ± 0.8/2.2 ± 0.9 for RGA. Visualization scores for the RGA were lower than for other hepatic arterial segments in both modalities, probably because of its small size and complex course. However, the overall visualization score of MSCTA was equivalent to that of DSA. MSCTA is advantageous in

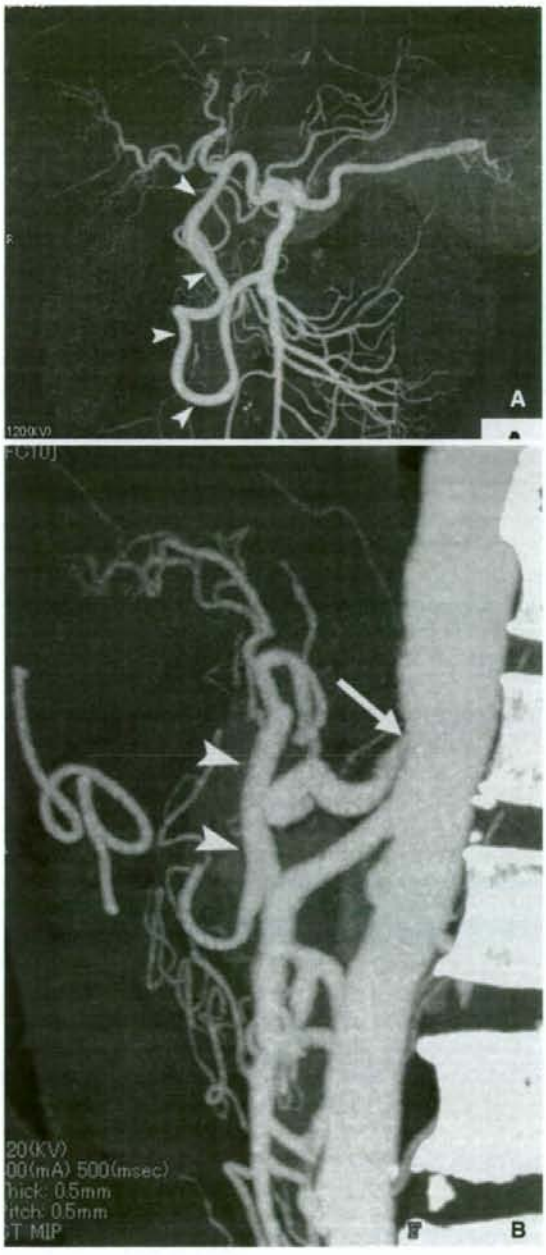

Fig. 5 Stenosis of the celiac trunk in a 57-year-old man with liver metastases. **A**, **B** Coronal (A) and sagittal (B) MPVR images show stenosis of the origin of the celiac trunk (arrows) and dilatation of the inferior pancreatic artery and the gastroduodenal artery (arrowheads)

giving information in advance of catheter and port placement, which may reduce the procedural time and avoid complications.

The course of the celiac axis also affects the technique of catheter placement. When a transfemoral or transepigastric approach is used, a caudal course of the celiac axis tends to be more difficult than a cranial course because multiple inflection points result in a reduction in torque of the catheter and guide wire. When the course is caudal, use of a specific J-type long sheath is considered for implantation of the catheter and port system [18]. Evaluation of the celiac axis prior to catheter and port implantation is important for planning the procedure. In this study, respiratory phase was consistent with routine examination and different between MSCTA and DSA. Lee et al. reported that there was no significant difference between inspiration and expiration in the angles between the celiac trunk and the aorta on MRI [19]. Factors other than respiration, such as redundant and tortuous celiac axis, may have affected the difference in our study. Even considering the effect of respiration, MSCTA showed an advantage in detecting the origin of the celiac trunk from the aorta constantly. Celiac DSA did not always demonstrate the origin of the celiac trunk. The 3-D capability of MSCTA is also effective for visualization of the celiac trunk from various directions.

Another important indication of preoperative vascular evaluation for HAIC is to detect vascular abnormalities such as stenosis or occlusion along the implantation route. Stenosis or occlusion may result not only in complications during procedures of angiography and catheter implantation, but also in early occlusion of the hepatic artery after catheter placement. In a postprocedure setting, MSCTA with intra-arterial administration of contrast material from an implanted catheter and port system help detect arterial stenosis [20]. In the present study, MSCTA with intravenous administration of contrast material demonstrated stenosis in two patients. In one patient with severe stenosis of the common stem of the celiac and mesenteric arteries, in which even diagnostic angiography poses a risk of complication, we could preclude angiography and catheter placement based on MSCTA findings.

In our series, interventional radiological placement of the catheter and port system was successful in all patients with preprocedural planning by MSCTA. Previously, we performed two sessions of DSA occasionally, one for evaluation of vascular anatomy and partial embolization and the other for placement of the catheter and port system and embolization. After implementation of MSCTA, this procedure has been done in one session, which may result in a shorter hospital stay.

Optimization of the radiation dose is crucial for MSCTA. In the current study, the radiation dose represented by CTDIvol and DLP was equivalent to the criteria from the European Guidelines on Quality Criteria for CT: weighted CTDI of 35 mGy and weighted DLP of 780 mGy · cm [21]. Although the radiation dose was not as low as in

the previous report of a spiral and conventional CT study [22], our result is acceptable because this examination is designed for single, not repeated, preprocedural assessment including evaluation of liver tumor, nodal, and peritoneal tumor extent. Furthermore, MSCTA images provide adequate information on vascular mapping, and they lead to an overall reduction of radiation dose. Nonetheless, further radiation dose reduction should be made, while maintaining image quality. Techniques to reduce the radiation dose include reducing the milliampere-second value, increasing the pitch, adjusting the milliampere-second value according to the patient's size, and reducing the beam energy [11, 23]. More important is to eliminate unnecessary CT examination or excessive multiphase study.

Limitations of our study include the small number of patients and lack of comparison with other noninvasive modalities such as duplex US. At our institute, contrast-enhanced CT is routinely used for pretreatment evaluation of malignant hepatic tumors and additional MSCTA in the same study was considered to be adequate. Another limitation is that we did not evaluate diverse reformation techniques for MSCTA, such as volume rendering (VR). We chose the MPVR technique based on our previous experience and reports by other investigators [9, 18, 24]. The application of target VR eliminated partial volume averaging on MPVR. This technique was useful in the visualization of small arteries such as the RGA, however, other reformation techniques should be taken into consideration.

In conclusion, MSCTA is accurate in the detection of abdominal arterial anatomy, variations, and abnormalities. MSCTA is suitable for planning of the catheter and port system implantation for HAIC.

Acknowledgment We are grateful to the Japanese Society of Implantable Port Assisted Regional Treatments (JSIPART) for awarding and supporting this study.

References

1. Arai Y, Inaba Y, Takeuchi Y (1997) Interventional techniques for hepatic arterial infusion chemotherapy. In: Casterneda-Zuniga E (ed) Interventional radiology. Williams & Wilkins, Baltimore, pp 192–205
2. Kemeny NE, Ron IG (1999) Hepatic arterial chemotherapy in metastatic colorectal patients. Semin Oncol 26:524–535
3. Tanaka T, Arai Y, Inaba Y, et al. (2003) Radiologic placement of side-hole catheter with tip fixation for hepatic arterial infusion chemotherapy. J Vasc Interv Radiol 14:63–68
4. Meta-Analysis Group in Cancer (1996) Meta-Analysis Group in Cancer: reappraisal of hepatic arterial infusion in the treatment of nonresectable liver metastases from colorectal cancer. J Natl Cancer Inst 88:252–258
5. Kemeny N, Niedzwiecki D, Hollis DR (2006) Hepatic arterial infusion versus systemic therapy for hepatic metastases from colorectal cancer: a randomized trial of efficacy, quality of life, and molecular markers (CALGB 9481). J Clin Oncol 24:1395–1403
6. Seki H, Kimura M, Yoshimura N, et al. (1999) Hepatic arterial infusion chemotherapy using percutaneous catheter placement with an implantable port: assessment of factors affecting patency of the hepatic artery. Clin Radiol 54:221–227
7. Guiney MJ, Kruskal JB, Sosna J, et al. (2003) Multi-detector row CT of relevant vascular anatomy of the surgical plane in split-liver transplantation. Radiology 229:401–407
8. Sahani D, Saini S, Pena C, et al. (2002) Using multidetector CT for preoperative vascular evaluation of liver neoplasms: technique and results. AJR 179:53–59
9. Byun JH, Kim TK, Lee SS, et al. (2003) Evaluation of the hepatic artery in potential donors for living donor liver transplantation by computed tomography angiography using multidetector-row computed tomography: comparison of volume rendering and maximum intensity projection techniques. J Comput Assist Tomogr 27:125–131
10. Takahashi S, Murakami T, Takamura M, et al. (2002) Multidetector row helical CT angiography of hepatic vessels: depiction with dual-arterial phase acquisition during single breath hold. Radiology 222:81–88
11. McNitt-Gray MF (2002) AAPM/RSNA physics tutorial for residents: topics in CT: radiation dose in CT. Radiographics 22:1541–1553
12. Erbay N, Raptopoulos V, Pomfret EA, et al. (2003) Living donor liver transplantation in adults: vascular variants important in surgical planning for donors and recipients. AJR 181:109–114
13. Fishman EK (2001) From the RSNA refresher courses: CT angiography: clinical applications in the abdomen. Radiographics 21:3–16
14. Winter TC III, Nghiem HV, Freeny PC, et al. (1995) Hepatic arterial anatomy: demonstration of normal supply and vascular variants with three-dimensional CT angiography. Radiographics 15:771–780
15. Sahani DV, Krishnamurthy SK, Kalva S, et al. (2004) Multidetector-row computed tomography angiography for planning intra-arterial chemotherapy pump placement in patients with colorectal metastases to the liver. J Comput Assist Tomogr 28:478–484
16. Kapoor V, Brancatelli G, Federle MP, et al. (2003) Multidetector CT arteriography with volumetric three-dimensional rendering to evaluate patients with metastatic colorectal disease for placement of a floxuridine infusion pump. AJR 181:455–463
17. Yamagami T, Nakamura T, Iida S, Kato T, Nishimura T (2002) Embolization of the right gastric artery before hepatic arterial infusion chemotherapy to prevent gastric mucosal lesions: approach through the hepatic artery versus the left gastric artery. AJR 179:1605–1610
18. Katoh K, Sone M, Nakasato T, et al. (2006) A new method using J-type long sheath for implantation of indwelling catheters for trans-femoral hepatic arterial infusion. Radiat Med 24:80–83
19. Lee VS, Morgan JN, Tan AGS, et al. (2003) Celiac artery compression by the median arcuate ligament: a pitfall of end-expiratory MR imaging. Radiology 228:437–442
20. Sone M, Kato K, Nakasato T, et al. (2002) Multislice CT angiography through an implantable catheter and port system: early experience in detection of vascular complications during hepatic arterial infusion chemotherapy. J Comput Assist Tomogr 26:515–519
21. European guidelines on quality criteria for computed tomography. Available at: http://www.drs.dk/guidelines/ct/quality/. Accessed December 12, 2006
22. Hidajat N, Wolf M, Nunnemann A, et al. (2001) Survey of conventional and spiral CT doses. Radiology 218:395–401
23. Karla MK, Maher MM, Toth TL, et al. (2004) Strategies for CT radiation dose optimization. Radiology 230:619–628
24. Mallouhi A, Rieger M, Czermak B, et al. (2003) Volume-rendered multidetector CT angiography: noninvasive follow-up of patients treated with renal artery stents. AJR 180:233–239